JACS
JOURNAL OF THE AMERICAN CHEMICAL SOCIETY
Article
pubs.acs.org/JACS

$Na_2ZnGe_2S_6$: A New Infrared Nonlinear Optical Material with Good Balance between Large Second-Harmonic Generation Response and High Laser Damage Threshold

Guangmao Li,[†,‡] Kui Wu,[*,†] Qiong Liu,[†,‡] Zhihua Yang,[†] and Shilie Pan[*,†]

[†]Key Laboratory of Functional Materials and Devices for Special Environments, Xinjiang Technical Institute of Physics & Chemistry, Xinjiang Key Laboratory of Electronic Information Materials and Devices, Chinese Academy of Sciences, 40-1 South Beijing Road, Urumqi 830011, China

[‡]University of Chinese Academy of Sciences, Beijing 100049, China

Supporting Information

ABSTRACT: The development of frequency-conversion technology in the infrared region is in urgent need of new excellent infrared nonlinear optical (IR NLO) materials. How to achieve a good balance between laser damage threshold (LDT) and NLO coefficient (d_{ij}) for new IR NLO candidates is still a challenge. The combination of the highly electropositive alkali metal (Na) and Zn with d^{10} electronic configuration into crystal structure affords one new IR NLO material, $Na_2ZnGe_2S_6$. It exhibits excellent properties including a wide transparent region (0.38−22 μm), large band gap (3.25 eV), and especially a balance between a strong NLO coefficient (30-fold that of KDP) and a high LDT (6-fold that of $AgGaS_2$), indicating a promising application in the IR region. Moreover, novel common-vertex-linked wavelike $_\infty[GeS_3]_n$ chains are interestingly discovered in $Na_2ZnGe_2S_6$, which rarely exist in the reported thiogermanides containing alkali metals. In addition, calculated SHG density and dipole moment demonstrate that the large NLO response is mainly attributed to the cooperative effects of the $[GeS_4]$ and $[ZnS_4]$ units.

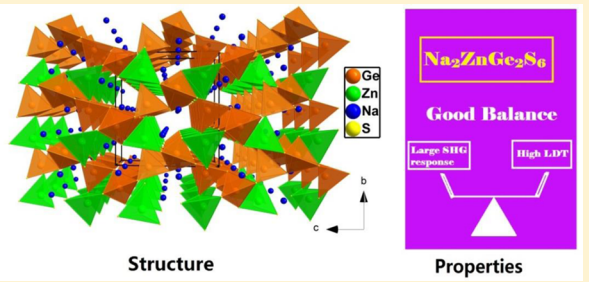

INTRODUCTION

Nonlinear optical (NLO) materials have attracted unprecedented attention in laser science and technology with the property of frequency conversion in solid-state lasers.[1−5] As is well-known, an excellent NLO material should involve the following important prerequisites: large SHG response, broad band gap (E_g), wide optical transparent region, chemical stability, and ability to obtain large single crystals. In the UV and visible regions, great achievements have been made by providing many excellent materials such as β-BaB_2O_4 (BBO), LiB_3O_5 (LBO), and $KBe_2BO_3F_2$ (KBBF).[6−10] In addition, in the infrared (IR) region (2−20 μm), many important fields including optoelectronic devices, resource exploration, and long-distance laser communication have drawn considerable attention and interests.[11−16] Commercial IR NLO materials, including $AgGaX_2$ (X = S and Se)[17] and $ZnGeP_2$,[18] exhibit good SHG coefficients for the application in IR region, but they are still defective in the high-power laser system owing to their low laser damage thresholds (LDT) or two-photon absorption, principally caused by the small E_g.[11c,19] Thus, searching for new materials with large LDTs and good NLO coefficients (d_{ij}) is an urgent need the for IR NLO field. However, general knowledge indicates that a large E_g is conducive to obtain the high LDT, but has an inverse proportion with d_{ij} in one NLO material.[20] Therefore, how to design and achieve a subtle balance of major properties (especially E_g and d_{ij}) for one promising IR NLO material is of great importance in laser science and technology. Guided by this purpose, hundreds of IR NLO metal halides, chalcogenides, and phosphides[21−23] have been discovered, and many materials exhibit excellent performances such as $Na_2Ge_2Se_5$ (371.8 × KDP, E_g = 2.38 eV),[23] $Ba_8Sn_4S_{15}$ (110.9 × KDP, E_g = 1.66 eV),[24] $AgGaTe_2$ (84 × KDP, E_g = 1.36 V),[25] $LiInSe_2$ (79.5 × KDP, E_g = 2.86 eV),[26] $K_2P_2Se_6$ (69 × KDP, E_g = 2.08 eV),[27] $BaGa_4Se_7$ (52.8 × KDP, E_g = 2.64 eV),[28] $LiGaGe_2Se_6$ (47.4 × KDP, E_g = 2.08 eV),[29] Li_2CdSnS_4 (2.56 × KDP, E_g = 3.26 eV),[30] $Cs_2HgCl_2I_2$ (1 × KDP, E_g = 3.15 eV),[31] and $Rb_2CdBr_2I_2$ (4 × KDP, E_g = 3.35 eV),[32] among others. However, up to now, only a few of them can achieve the balance (d_{ij} > 3.9 pm/V and E_g > 3.0 eV) demanded by excellent IR NLO materials. Moreover, through the overall investigation on the reported crystal structures, it can be found that highly electropositive alkali or alkaline earth metals and $M^{IV}S_4$ (M^{IV} = Si, Ge, and Sn) units appear more frequently.[33,34] Besides, introduction of the d^{10} cations with relatively small covalent radius (such as Zn^{2+}) into the crystal structure can also increase the E_g and maintain the relatively large d_{ij}, such as $Zn_3(PS_4)_2$ and $LiZnPS_4$.[19,35] Accordingly, by combining the

Received: April 12, 2016
Published: May 19, 2016

DOI: 10.1021/jacs.6b03734
J. Am. Chem. Soc. 2016, 138, 7422−7428

highly electropositive Na and d^{10} Zn elements with distorted GeS_4 units, a new IR NLO material, $Na_2ZnGe_2S_6$, was successfully synthesized. It exhibits excellent properties: good NLO coefficient (~30 × KDP), high LDT (6 × benchmark $AgGaS_2$), large band gap (3.25 eV), broad transparent region (0.38−22 μm), and specially a good balance between E_g and d_{ij}, which shows it is a good candidate with promising application in the IR NLO field. Moreover, both the SHG density and dipole moment calculation demonstrate that its SHG response originates from the cooperative contribution made by the $[GeS_4]$ and $[ZnS_4]$ units.

EXPERIMENTAL SECTION

Synthesis. All the elementary substances (with the purities higher than 99.99%) were purchased from Shanghai Aladdin Biochemistry Technology Co., Ltd., and then stored in a dry Ar-filled glovebox without oxygen and moisture. The crystals of $Na_2ZnGe_2S_6$ were synthesized by solid-state reaction as follows: (1) Na, Zn, Ge, and S with stoichiometric ratio were loaded into a 7 mm (inner diameter) graphite crucible. (2) The crucible was removed into a 10 mm (inner diameter) fused-silica tube under an Ar atmosphere in a glovebox. (3) The silica tube was sealed with methane−oxygen flame under a high vacuum of 10^{-3} Pa. (4) Then, the tube was placed in a computer-controlled furnace, heated to 700 °C in 50 h, dwelled at 700 °C for 100 h, cooled to 200 °C at a rate of 5 K/h, and finally cooled to room temperature by switching off the furnace. After that, colorless $Na_2ZnGe_2S_6$ single crystals with the largest size up to millimeter level were obtained.

Powder X-ray Diffraction. The microcrystalline powders used for various experiments were prepared by grinding the single crystals after washing with N,N-dimethylformamide (DMF). Powder X-ray diffraction analysis was performed at 298 K in the angular range of 2θ = 10−70°, with a scan step width of 0.02° and a fixed counting time of 1 s/step using an automated Bruker D2 X-ray diffractometer equipped with a diffracted monochromator set for Cu KR (λ = 1.5418 Å) radiation. The experimental X-ray diffraction pattern matches well with the calculated one that is generated using the Mercury program with CIF data.

Single-Crystal X-ray Crystallography. A transparent colorless crystal was first selected under a microscope and mounted on the top of a glass fiber with epoxy. Structure data were collected with a Bruker SMART APEX II 4K CCD diffractometer that was equipped with Mo Kα radiation (λ = 0.71073 Å) operating at 50 kV and 40 mA at 296(2) K. The structure determination is based on direct method, and the data were refined through full-matrix least-squares on F^2 using SHELXTL program package.[36] Program XPREP was applied for face-indexed absorption. The structures were checked with PLATON[37] in case of additional symmetry elements, and no higher symmetries were provided. Details of data collection, structure refinements, and crystal parameters are given in Table 1. The equivalent isotropic displacement parameters and atomic coordinates are summarized in Table S1, and selected bond lengths and angles are listed in Table S2.

Infrared Spectrum. The IR spectrum was recorded on a Shimadzu IRAffinity-1 Fourier transform infrared spectrometer with a resolution of 2 cm^{-1}, covering the wavenumber range of 400−4000 cm^{-1}. The crystal samples and KBr were mixed in the ratio of about 1:100, dried, and ground into fine powder and then pressed into a transparent sheet on the tablet machine. The sheet was loaded in the sample chamber, and then the IR spectrum was measured.

UV−Vis−NIR Diffuse Reflectance Spectroscopy. Optical diffuse reflectance spectrum of $Na_2ZnGe_2S_6$ was measured at 298 K with Shimadzu SolidSpec-3700DUV spectrophotometer. Spectral data were collected with a wavelength range of 190−2600 nm, which would provide the visible or UV cutoff edge. The data of reflectance spectra were converted to absorbance using the Kubelka−Munk function[38] to estimate the band gap.

Raman Spectroscopy. The Raman spectrum was collected with crushed crystal on a LABRAM HR Evolution spectrometer equipped with a CCD detector using 532 nm radiation from a diode laser. Crystals were selected and loaded on a glass slide; then, a 50× objective lens was used to choose the area to be measured on the crystal. A beam with the diameter of 35 μm and maximum power of 60 mW was used, and spectrum data collection was finished in 15 s.

Table 1. Crystal Data and Structure Refinement for $Na_2ZnGe_2S_6$

empirical formula	$Na_2ZnGe_2S_6$
formula weight	448.89
temperature	296(2) K
wavelength	0.71073 Å
crystal system, space group	*Cc*
unit cell dimensions	a = 7.284(9) Åa = 7.284(9) Å b = 12.346(15) Åb = 12.346(15) Å c = 11.447(14) Åc = 11.447(14) Å β = 100.627(13)°β = 100.627(13)°
volume	1012(2) Å^{3}1012(2) Å^3
Z (calculated density)	4 (2.947 kg/m^3)
absorption coefficient	9.507 mm^{-1}
F(000)	848
crystal size	0.235 × 0.135 × 0.116 mm^3
theta range for data collection	3.29−27.40°
limiting indices	$-9 \le h \le 9$, $-15 \le k \le 9$, $-14 \le l \le 14$
reflections (collected/unique)	2962/1887 [$R_{(int)}$ = 0.0382]
completeness to theta = 27.40	98.8%
refinement method	full-matrix least-squares on F^2
data/restraints/parameters	1887/2/100
goodness-of-fit on F^2	0.970
final R indices [$I > 2\varsigma(I)$]	R_1 = 0.0374, wR_2 = 0.0645
R indices (all data)	R_1 = 0.0435, wR_2 = 0.0673
absolute structure parameter	0.023(17)
largest diff. peak and hole	0.738 and −0.773 e·Å^{-3}

Second-Harmonic Generation. The SHG response measurement was performed by the Kurtz and Perry method with a 2.09 μm Q-switch laser.[39] The crystals were ground and sieved into five particle size ranges of 55−88, 88−105, 105−150, 150−200, and 200−250 μm, with microcrystalline $AgGaS_2$ of the same particle size ranges serving as references. The samples were placed on a glass microscope cover slide, secured by a 1 mm thick silicone insole with an 8 mm diameter hole, and then covered with another glass slide. Then, they were placed into light-tight boxes and explored under a pulsed infrared beam from a Q-switched Ho:Tm:Cr:YAG laser with wavelength of 2.09 μm. The SHG signals were recorded on the oscilloscope that was connected with the detector. The procedure was repeated using the standard IR NLO material of $AgGaS_2$.

LDT Measurement. LDT was measured using a 1064 nm Q-switch laser on a ground powder of $Na_2ZnGe_2S_6$ crystals and $AgGaS_2$ as a reference. The samples were surrounded by a 1 mm thick silicone pad with an 8 mm diameter hole and pressed between two glass slides. Then, they were fixed in a light-tight box with the plane surface explored under a pulsed laser beam (1064 nm, 10 ns). The pulse energy was raised from 0.2 mJ and stopped when obvious damage is discovered under a microscope after the irradiation.

Theoretical Calculations. The first-principle calculations for the experimental crystal structure were obtained on the basis of ab initio calculations implemented in the CASTEP package through density functional theory (DFT).[40] The generalized gradient approximation (GGA) was adopted, and Perdew−Burke−Ernzerhof (PBE) functional was chosen to calculate the exchange-correlation potential, with an energy cutoff of 900.0 eV. The k integration over the Brillouin zone was performed by the tetrahedron method[41] using a Monkhorst−Pack grid of 4 × 4 × 2. Because the discontinuity of exchange correlation

DOI: 10.1021/jacs.6b03734
J. Am. Chem. Soc. 2016, 138, 7422−7428

energy may lead to a smaller band gap than the experimental value, a scissors operator[42] was used in these calculations.

The SHG coefficients calculations are performed on the basis of the band wave functions by using the so-called length-gauge formalism derived by Aversa and Sipe[43] at a zero frequency limit. The static second-order nonlinear susceptibilities $\chi_{\alpha\beta\gamma}^{(2)}$ can be simplified as[44]

$$\chi_{\alpha\beta\gamma}^{(2)} = \chi_{\alpha\beta\gamma}^{(2)}(\mathrm{VE}) + \chi_{\alpha\beta\gamma}^{(2)}(\mathrm{VH}) + \chi_{\alpha\beta\gamma}^{(2)}(\text{two bands})$$

In this sum-overstates type formalism, the total SHG coefficient $\chi^{(2)}$ is divided into contributions from virtual-hole (VH), virtual-electron (VE), and two-band (TB) processes. On the basis of this, we calculated the origin of the SHG coefficient.

RESULTS AND DISCUSSIONS

Crystal Growth. Single crystals of $Na_2ZnGe_2S_6$ with a size of up to a millimeter level were successfully synthesized by solid-state reaction technique in a fused-silica tube. They are colorless and transparent; the photograph of crystals in millimeter level (the largest one is 1.5 × 1.5 × 0.5 mm^3) is shown in Figure 1. The crystals exist stably in air for half a year

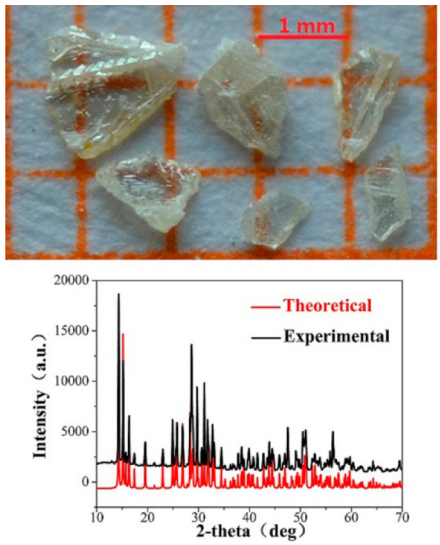

Figure 1. Upper panel, photograph of the $Na_2ZnGe_2S_6$ crystals; lower panel, powder XRD patterns of $Na_2ZnGe_2S_6$.

without weight loss and appearance change. Powder X-ray diffraction analysis was performed with the microcrystal of $Na_2ZnGe_2S_6$, and the experimental and theoretical XRD spectra match well (shown in Figure 1), which demonstrates the purity of the compound.

Crystal Structure. Single-crystal structural analysis shows that this compound crystallizes in noncentrosymmetric (NCS) space group *Cc* (no. 9) with the unit cell parameters of *a* = 7.284(9) Å, *b* = 12.346(15) Å, *c* = 11.447(14) Å, *β* = 100.63°, and *Z* = 4. In its asymmetric structure, there are two crystallographically unique Na atoms, one Zn atom, two Ge atoms, and six S atoms. Its structure is composed of two different 3D tunnel frameworks: one of infinite $_\infty[GeS_3]_n$ chains and isolated $[ZnS_4]$ tetrahedra (shown in Figure 2a), and the other with corner-shared $Na(1)S_5$ polyhedra and $Na(2)S_6$ octahedra (Figure 2b). The two 3D frameworks insert the tunnels of each other and compose an integrated 3D network. Each of the Ge atoms link with four S atoms to form typical $[GeS_4]$ tetrahedra with the *d*(Ge−S) = 2.162−2.265 Å, and then the $[GeS_4]$ tetrahedra connect with each other by

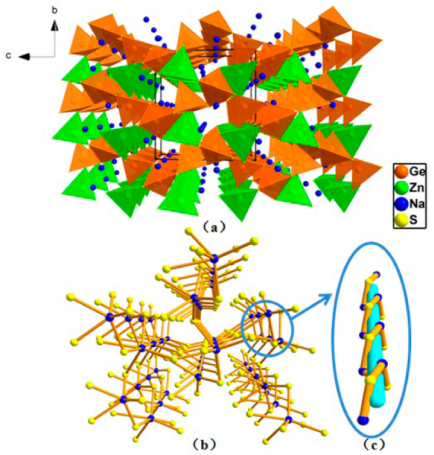

Figure 2. (a) 3D tunnel structure of $Na_2ZnGe_2S_6$ formed by $_\infty[GeS_3]_n$ chains, isolated $[ZnS_4]$, and charge-balanced Na cations along *a* axis; (b) a 3D framework structure composed of the $Na(1)S_5$ and $Na(2)S_6$ units; (c) a Na(1)−S−Na(2) spiral chain along *a* axis.

sharing corners to make up isolated wavelike $_\infty[GeS_3]_n$ chains. Moreover, the Zn atoms are connected with four S atoms with *d*(Zn−S) = 2.342−2.357 Å to form the $[ZnS_4]$ tetrehadra, which act as the connections between the wavelike infinite $_\infty[GeS_3]_n$ chains, and they build up a tunnel 3D framework. The Na atoms locate in the tunnels and have two different coordination environments, including highly distorted $Na(1)S_5$ polyhedra with *d*(Na−S) = 2.782−3.029 Å and $Na(2)S_6$ octahedra with *d*(Na−S) = 2.773−3.284 Å. Note that the $Na(1)S_5$ and $Na(2)S_6$ units in the same tunnel connect with each other alternately by sharing corners to form $[Na(1)-S-Na(2)]_n$ spiral chains along the *a* axis as shown in Figure 2c, and these chains in different tunnels interlink with each other through S atoms to make up another tunnel 3D framework.

In most of the alkali-containing thiogermanides,[45] the $[GeS_4]$ units exist in isolation or reunite to form $[Ge_2S_6]$, $[Ge_3S_9]$, or $[Ge_4S_{10}]$ units similar to that in $K_2PbGe_2S_6$,[46] $Na_2Ge_2S_5$,[47] and $K_2Ge_2S_5$,[48] respectively. In addition, although there the $_\infty[GeS_3]_n$ chains exist in $Cs_2ZnGe_3S_8$ and $Cs_2CdGe_3S_8$,[49] they are connected by sharing corners and edges alternatively and are not common-vertex-linked. Thus, the common-vertex-linked $_\infty[GeS_3]_n$ chains for the title compound are rarely found Na_2GeS_3[45h] in the thiogermanides containing alkali metal.

Optical Properties. The IR and UV−vis−NIR diffuse reflection spectral measurements were recorded, and the results show that $Na_2ZnGe_2S_6$ exhibits a wide transparent region of 0.38−22 μm (Figure 3), which covers the two important atmospheric transparent windows (3−5 and 8−12 μm). Some other IR NLO powdered compounds have comparable IR absorption edges with $Na_2ZnGe_2S_6$, such as $AgGaS_2$ (~23 μm),[17a] $BaGa_4Se_7$ (~18 μm),[28] Li_2CdGeS_4 (~22 μm),[34] and $CsCd_4Ga_5S_{12}$ (~25 μm).[50] The Raman spectrum (shown in Figure S1) also shows no absorption peaks in the region of 450−1000 cm^{-1} (10−22 μm), which further proves that $Na_2ZnGe_2S_6$ has a wide IR transmission region. Moreover, experimental E_g of $Na_2ZnGe_2S_6$ is 3.25 eV, which is much larger than that of the commercial crystals $AgGaS_2$ (2.56 eV) and $AgGaSe_2$ (1.83 eV) and comparable to that of several outstanding materials, such as $LiInS_2$ (3.57 eV),[26a] $BaGa_4S_7$ (3.54 eV),[21a] and Li_2CdGeS_4 (3.15 eV).[30]

DOI: 10.1021/jacs.6b03734
J. Am. Chem. Soc. 2016, 138, 7422−7428

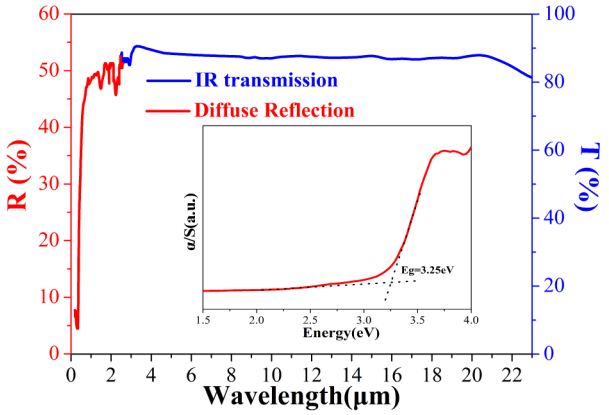

Figure 3. Optical spectra of $Na_2ZnGe_2S_6$. The inserted diagram is the experimental band gap.

As is well-known, strong photon absorption can result in electronic and thermal effects, which may further lead to laser damage for one material. A large optical band gap generally improves the difficulty of photon absorption and then corresponds to high LDT. $Na_2ZnGe_2S_6$ exhibits a large band gap (E_g = 3.25 eV), which prompts us to measure its LDT, so the powder LDT of $Na_2ZnGe_2S_6$ (ground $AgGaS_2$ single crystals as the reference) was measured on the basis of a Q-switched pulse laser (1064 nm, 10 ns, 10 Hz). The results show that $Na_2ZnGe_2S_6$ has a high LDT of 228 MW/cm^2, about 6 times that of benchmark $AgGaS_2$ (37 MW/cm^2). Note that the measured LDT of $AgGaS_2$ in this work is larger than that in our previous work,[4h] which is induced by the different measured samples (single crystals in this work vs polycrystalline samples in our previous work). It is obvious that $Na_2ZnGe_2S_6$ obtains a high LDT that optimizes the drawback of $AgGaS_2$ and finally realizes a balance between large SHG response and high LDT.

Searching for an excellent IR NLO material with high LDT while maintaining moderate SHG response is challenging and urgent. SHG coefficient as another important parameter is also studied with a 2.09 μm Q-switch laser in different particle sizes (shown in Figure 4a). The results show that it is type I phase-matchable and exhibits SHG efficiency, which is 0.9 times that of $AgGaS_2$ at the maximum particle size (shown in Figure 4b). In general, the SHG coefficient of powder $AgGaS_2$ is about 33 times of that of KDP, so this compound exhibits a large SHG coefficient about 30 times that of KDP, comparable to that of the famous material $BaGa_4S_7$,[21a] which indicates that it has a promising application in the IR NLO field.

For comparisons, the properties of $AgGaS_2$, $LiInS_2$, $LiGaS_2$, $BaGa_4S_7$, $Rb_2CdBr_2I_2$, and $Na_2ZnGe_2S_6$ were shown in Table 2.

Table 2. Properties Comparison among $AgGaS_2$, $LiInS_2$, $LiGaS_2$, $BaGa_4S_7$, $Rb_2CdBr_2I_2$, and $Na_2ZnGe_2S_6$

formula	E_g (eV)	d_{ij} (× KDP)	LDT (× AGS)	trans. region (μm)
$AgGaS_2$[17]	2.64	33.3	1	0.41−12
$LiInS_2$[26a,b]	3.57	19	2.5	0.41−12
$LiGaS_2$[26a,c]	4.15	15	11	0.32−11.6
$BaGa_4S_7$[21a]	3.54	33.3	3	0.35−13.7
$Rb_2CdBr_2I_2$[32]	3.35	4	6	0.37−14
$Na_2ZnGe_2S_6$	3.25	30	6	0.38−22

From the table, it is obviously found that $Na_2ZnGe_2S_6$ exhibits excellent optical properties and especially satisfies the good balance between large d_{ij} and high LDT as a promising IR NLO candidate.

Theoretical Studies. To achieve a deep investigation about structure−property relationship, theoretical calculations based on DFT methods were performed. The calculated band structures (Figure 5a) show that $Na_2ZnGe_2S_6$ is a direct band gap material with a theoretical band gap about 2.63 eV, smaller than the experimental result (3.25 eV), owing to the common underestimation of E_g by the DFT method.

The total and partial density of states (TDOS and PDOS) diagram of $Na_2ZnGe_2S_6$ is shown in Figure 5b. The upper part of valence bond (near Fermi level) is mainly composed of the Zn 3p, Ge 4p, and S 3p states. The bottom of the conduction bond region is mainly from the Ge 4s,4p, Zn 3p, Na 2p,3s, and S 3p states. Accordingly, the S 3p and Ge 4s orbitals determine the optical band gap of $Na_2ZnGe_2S_6$, and the optical absorption may be determined by the [GeS_4] and [ZnS_4] units.

$Na_2ZnGe_2S_6$ belongs to *Cs* point symmetry and has six independent SHG coefficients, and the results show that d_{11} = −4.3 pm/V, d_{12} = 4.63 pm/V, d_{13} = −5.3 pm/V, d_{15} = −4.3 pm/V, d_{24} = 4.63 pm/V, and d_{33} = −5.3 pm/V, respectively. Furthermore, the birefringence is also calculated to be about 0.026 at 1.06 μm, as shown in Figure S2. In addition, the SHG density diagram was also calculated with electron-including occupied and unoccupied states. The results show that the [GeS_4] and [ZnS_4] units make the main contribution to the SHG coefficient (Figure 6), which is coincident with the dipole

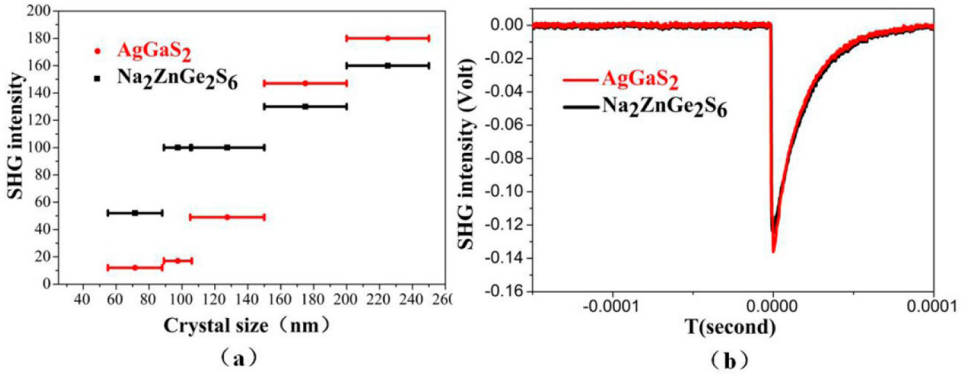

Figure 4. (a) SHG intensities of $Na_2ZnGe_2S_6$ and $AgGaS_2$ at 2.09 μm. (b) Comparison of SHG intensity of $Na_2ZnGe_2S_6$ and $AgGaS_2$ at the particle size of 200−250 μm.

DOI: 10.1021/jacs.6b03734
J. Am. Chem. Soc. 2016, 138, 7422−7428

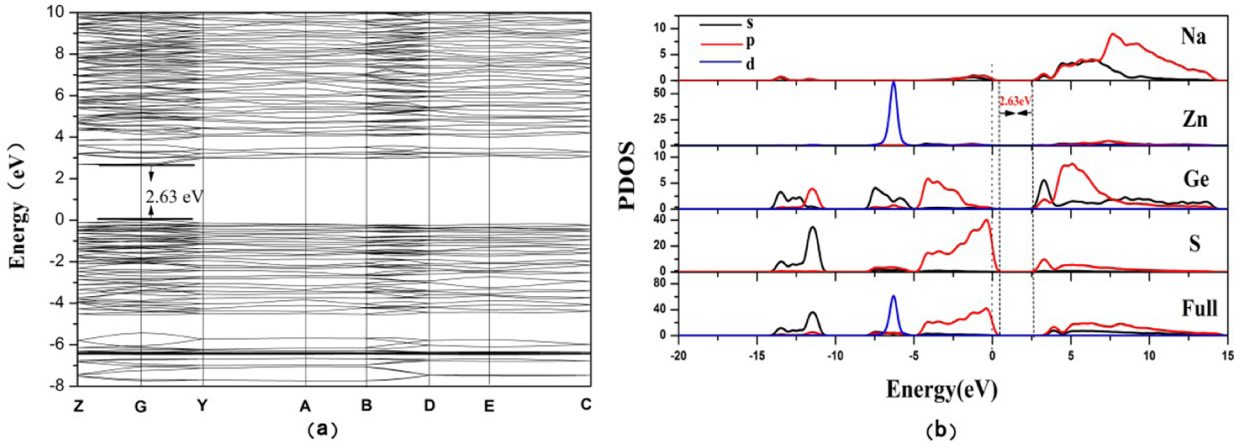

Figure 5. (a) Band structure of $Na_2ZnGe_2S_6$. (b) TDOS and PDOS plots of $Na_2ZnGe_2S_6$.

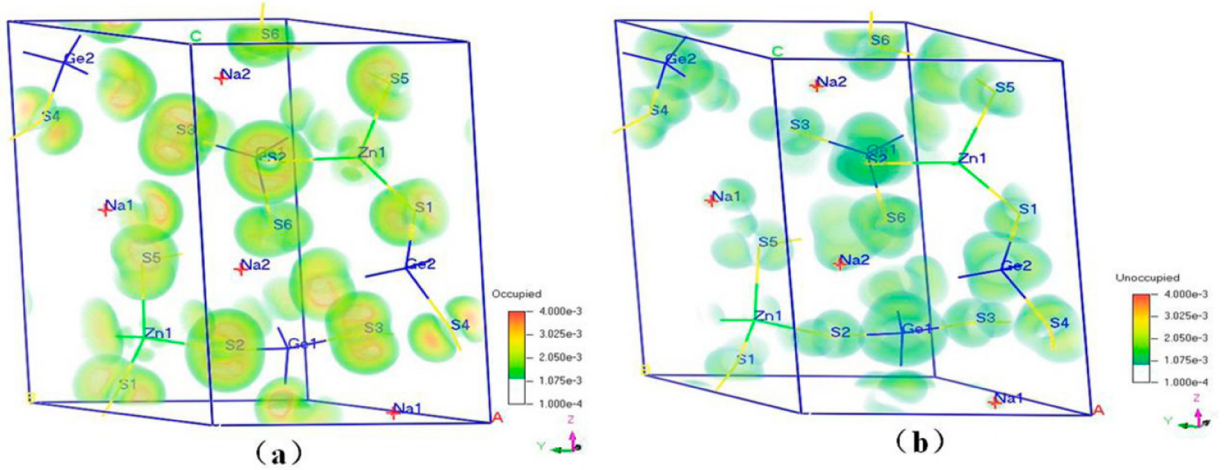

Figure 6. (a) SHG density of $Na_2ZnGe_2S_6$ at the occupied state. (b) SHG density of $Na_2ZnGe_2S_6$ at the unoccupied state.

moment calculation results (shown in Table S3), $\mu(Ge(1)S_4)$ = 67.7 debye, $\mu(Ge(2)S_4)$ = 76.4 debye, and $\mu(ZnS_4)$ = 51.6 debye, whereas the results of dipole moment calculations for $Na(1)S_5$ and $Na(2)S_6$ are both smaller than 30 debye. Therefore, both the dipole moment calculation and the SHG density calculation demonstrate that the $[GeS_4]$ and $[ZnS_4]$ units are the main origin of the SHG coefficient.

CONCLUSIONS

$Na_2ZnGe_2S_6$, a new IR NLO material, has been successfully synthesized with solid-state reaction technique in fused-silica tubes. Its structures are composed of two 3D tunnel frameworks, one constructed by polar wave-shaped infinite $_\infty[GeS_3]_n$ chains and isolated $[ZnS_4]$ tetrahedra and the other constructed by the $Na(1)S_5$ and $Na(2)S_6$ polyhedra. Remarkably, it exhibits not only wide transparent region (0.38−22 μm), large direct band gap (3.25 eV), and chemical stability but also achieves the balance between large LDT (228 MW/cm^2, about 6-fold that of $AgGaS_2$) and large SHG response (30-fold that of KDP). Moreover, single crystals of $Na_2ZnGe_2S_6$ have been obtained with a size up to millimeter level. Calculated SHG density and dipole moment demonstrate that the good SHG response is mainly attributed to the cooperative effects of the $[GeS_4]$ and $[ZnS_4]$ units; TDOS and PDOS diagrams present that it has a direct band gap and that the optical absorption is determined by the $[GeS_4]$ and $[ZnS_4]$ units. All the properties, especially the balance between large SHG response and high LDT, indicate that it has the potential to be a candidate crystal applied in the IR NLO region, and we will pay more attention to growing large single crystals for evaluating this application in the future.

ASSOCIATED CONTENT

Supporting Information

The Supporting Information is available free of charge on the ACS Publications website at DOI: 10.1021/jacs.6b03734.

Atomic coordinates and isotropic displacement parameters; selected bond distances and angles; Raman spectrum; local dipole moment calculation (PDF)

Crystallographic information file for $Na_2ZnGe_2S_6$ (CIF)

AUTHOR INFORMATION

Corresponding Authors

*E-mail: slpan@ms.xjb.ac.cn.

*E-mail: wukui@ms.xjb.ac.cn.

Notes

The authors declare no competing financial interest.

DOI: 10.1021/jacs.6b03734
J. Am. Chem. Soc. 2016, 138, 7422−7428

■ ACKNOWLEDGMENTS

This work was supported by the Xinjiang Program of Cultivation of Young Innovative Technical Talents (Grant No. 2014731029), the Western Light Foundation of CAS (Grant No. XBBS201318), the National Natural Science Foundation of China (Grant Nos. 51402352, 51425206, U1129301, and 51172277), the Xinjiang International Science & Technology Cooperation Program (20146001), the Special Fund for Xinjiang Key Laboratories (Grant No. 2014KL009), and the Science and Technology Project of Urumqi (Grant No. 51425206).

■ REFERENCES

(1) (a) Cyranoski, D. *Nature* **2009**, *457*, 953. (b) Becker, P. *Adv. Mater.* **1998**, *10*, 979. (c) Chang, H. Y.; Kim, S. H.; Halasyamani, P. S.; Ok, K. M. *J. Am. Chem. Soc.* **2009**, *131*, 2426. (d) Tran, T. T.; He, J. G.; Rondinelli, J. M.; Halasyamani, P. S. *J. Am. Chem. Soc.* **2015**, *137*, 10504. (e) Donakowski, M. D.; Gautier, R.; Yeon, J.; Moore, D. T.; Nino, J. C.; Halasyamani, P. S.; Poeppelmeier, K. R. *J. Am. Chem. Soc.* **2012**, *134*, 7679. (f) Nguyen, S. D.; Yeon, J.; Kim, S. H.; Halasyamani, P. S. *J. Am. Chem. Soc.* **2011**, *133*, 12422. (g) Song, S. Y.; Lee, D. W.; Ok, K. M. *Inorg. Chem.* **2014**, *53*, 7040. (h) Bae, S. W.; Kim, C. Y.; Lee, D. W.; Ok, K. M. *Inorg. Chem.* **2014**, *53*, 11328.

(2) (a) Cyranoski, D. *Nature* **2009**, *457*, 953. (b) Wang, S.; Ye, N.; Li, W.; Zhao, D. *J. Am. Chem. Soc.* **2010**, *132*, 8779. (c) Huppertz, H. *Chem. Commun.* **2011**, *47*, 131. (d) Huppertz, H.; von der Eltz, B. *J. Am. Chem. Soc.* **2002**, *124*, 9376. (e) Zhao, S. G.; Gong, P. F.; Bai, L.; Xu, X.; Zhang, S. Q.; Sun, Z. H.; Lin, Z. S.; Hong, M. C.; Chen, C. T.; Luo, J. H. *Nat. Commun.* **2014**, *5*, 4019. (f) Yu, P.; Wu, L. M.; Zhou, L. J.; Chen, L. *J. Am. Chem. Soc.* **2014**, *136*, 480. (g) Maggard, P. A.; Stern, C. L.; Poeppelmeier, K. R. *J. Am. Chem. Soc.* **2001**, *123*, 7742. (h) Donakowski, M. D.; Gautier, R.; Yeon, J.; Moore, D. T.; Nino, J. C.; Halasyamani, P. S.; Poeppelmeier, K. R. *J. Am. Chem. Soc.* **2012**, *134*, 7679.

(3) (a) Sun, C. F.; Hu, C. L.; Xu, X.; Yang, B. P.; Mao, J. G. *J. Am. Chem. Soc.* **2011**, *133*, 5561. (b) Xu, X.; Hu, C. L.; Li, B. X.; Yang, B. P.; Mao, J. G. *Chem. Mater.* **2014**, *26*, 3219. (c) Wu, Y. C.; Sasaki, T.; Nakai, S.; Yokotani, A.; Tang, H. G.; Chen, C. T. *Appl. Phys. Lett.* **1993**, *62*, 2614.

(4) (a) Pan, S. L.; Smit, J. P.; Watkins, B.; Marvel, M. R.; Stern, C. L.; Poeppelmeier, K. R. *J. Am. Chem. Soc.* **2006**, *128*, 11631. (b) Wu, H. P.; Pan, S. L.; Poeppelmeier, K. R.; Li, H. Y.; Jia, D. Z.; Chen, Z. H.; Fan, X. Y.; Yang, Y.; Rondinelli, J. M.; Luo, H. *J. Am. Chem. Soc.* **2011**, *133*, 7786. (c) Yu, H. W.; Pan, S. L.; Wu, H. P.; Zhao, W. W.; Zhang, F. F.; Li, H. Y.; Yang, Z. H. *J. Mater. Chem.* **2012**, *22*, 2105. (d) Wu, H. P.; Yu, H. W.; Yang, Z. H.; Hou, X. L.; Su, X.; Pan, S. L.; Poeppelmeier, K. R.; Rondinelli, J. M. *J. Am. Chem. Soc.* **2013**, *135*, 4215. (e) Yu, H. W.; Wu, H. P.; Pan, S. L.; Yang, Z. H.; Hou, X. L.; Su, X.; Jing, Q.; Poeppelmeier, K. R.; Rondinelli, J. M. *J. Am. Chem. Soc.* **2014**, *136*, 1264. (f) Dong, X. Y.; Jing, Q.; Shi, Y. J.; Yang, Z. H.; Pan, S. L.; Poeppelmeier, K. R.; Young, J.; Rondinelli, J. M. *J. Am. Chem. Soc.* **2015**, *137*, 9417. (g) Yu, H. W.; Zhang, W. G.; Young, J.; Rondinelli, J. M.; Halasyamani, P. S. *J. Am. Chem. Soc.* **2016**, *138*, 88. (h) Wu, K.; Yang, Z. H.; Pan, S. L. *Angew. Chem., Int. Ed.* **2016**, *55*, DOI: 10.1002/anie.201602317.

(5) (a) Liao, J. H.; Marking, G. M.; Hsu, K. F.; Matsushita, Y.; Ewbank, M. D.; Borwick, R.; Cunningham, P.; Rosker, M. J.; Kanatzidis, M. G. *J. Am. Chem. Soc.* **2003**, *125*, 9484. (b) Chung, I.; Malliakas, C. D.; Jang, J. I.; Canlas, C. G.; Weliky, D. P.; Kanatzidis, M. G. *J. Am. Chem. Soc.* **2007**, *129*, 14996. (c) Liao, J. H.; Marking, G. M.; Hsu, K. F.; Matsushita, Y.; Ewbank, M. D.; Borwick, R.; Cunningham, P.; Rosker, M. J.; Kanatzidis, M. G. *J. Am. Chem. Soc.* **2003**, *125*, 9484. (d) Bera, T. K.; Song, J. H.; Freeman, A. J.; Jang, J. I.; Ketterson, J. B.; Kanatzidis, M. G. *Angew. Chem., Int. Ed.* **2008**, *47*, 7828. (e) Li, L. Y.; Li, G. B.; Wang, Y. X.; Liao, F. H.; Lin, J. H. *Chem. Mater.* **2005**, *17*, 4174.

(6) (a) Smith, W. L. *Appl. Opt.* **1977**, *16*, 1798. (b) Kato, K. *IEEE J. Quantum Electron.* **1991**, *27*, 1137.

(7) (a) Boyd, G. D.; Miller, R. C.; Nassau, K.; Bond, W. L.; Savage, A. *Appl. Phys. Lett.* **1964**, *5*, 234. (b) Chen, C. T.; Wu, B. C.; Jiang, A. D.; You, G. M. *Sci. Sin., Ser. B (Engl. Ed.)* **1985**, *28*, 235.

(8) Chen, C. T.; Wu, Y. C.; Jiang, A. D.; Wu, B. C.; You, G. M.; Li, R. K.; Lin, S. J. *J. Opt. Soc. Am. B* **1989**, *6*, 616.

(9) Mori, Y.; Kuroda, I.; Nakajima, S.; Sasaki, T.; Nakai, S. *Appl. Phys. Lett.* **1995**, *67*, 1818.

(10) Xia, Y. N.; Chen, C. T.; Tang, D. Y.; Wu, B. C. *Adv. Mater.* **1995**, *7*, 79.

(11) (a) Wu, K.; Pan, S. L.; Yang, Z. H. *RSC Adv.* **2015**, *5*, 33646. (b) Wu, K.; Su, X.; Pan, S. L.; Yang, Z. H. *Inorg. Chem.* **2015**, *54*, 2772. (c) Zhang, H.; Zhang, M.; Pan, S. L.; Dong, X. Y.; Yang, Z. H.; Hou, X. L.; Wang, Z.; Chang, K. B.; Poeppelmeier, K. R. *J. Am. Chem. Soc.* **2015**, *137*, 8360.

(12) (a) Chen, L.; Corbett, J. D. *J. Am. Chem. Soc.* **2003**, *125*, 1170. (b) Chen, M. C.; Li, L. H.; Chen, Y. B.; Chen, L. *J. Am. Chem. Soc.* **2011**, *133*, 4617. (c) Lin, H.; Chen, L.; Zhou, L. J.; Wu, L. M. *J. Am. Chem. Soc.* **2013**, *135*, 12914. (d) Yu, P.; Zhou, L. J.; Chen, L. *J. Am. Chem. Soc.* **2012**, *134*, 2227.

(13) (a) Jiang, X. M.; Zhang, M. J.; Zeng, H. Y.; Guo, G. C.; Huang, J. S. *J. Am. Chem. Soc.* **2011**, *133*, 3410. (b) Geng, L.; Cheng, W. D.; Lin, C. S.; Zhang, W. L.; Zhang, H.; He, Z. Z. *Inorg. Chem.* **2011**, *50*, 5679. (c) Zhou, J.; Zhao, J. W.; Wei, Q.; Zhang, J.; Yang, G. Y. *J. Am. Chem. Soc.* **2014**, *136*, 5065.

(14) Serebryakov, V. A.; Boiko, E. V.; Petrishchev, N. N.; Yan, A. V. *J. Opt. Technol.* **2010**, *77*, 6.

(15) Bordui, P. F.; Fejer, M. M. *Annu. Rev. Mater. Sci.* **1993**, *23*, 321.

(16) Pushkarsky, M. B.; Webber, M. E.; Macdonald, T.; Patel, C. K. N. *Appl. Phys. Lett.* **2006**, *88*, 044103.

(17) (a) Okorogu, A. O.; Mirov, S. B.; Lee, W.; Crouthamel, D. I.; Jenkins, N.; Dergachev, A. Y.; Vodopyanov, K. L.; Badikov, V. V. *Opt. Commun.* **1998**, *155*, 307. (b) Boyd, G. D. *Appl. Phys. Lett.* **1971**, *18*, 301. (c) Dmitriev, V. G.; Gurzadyan, G. G.; Nikogosyan, D. N. *Handbook of Nonlinear Optical Crystals*, 3rd ed.; Springer: New York, 1999.

(18) Jackson, A. G.; Ohmer, M. C.; LeClair, S. R. *Infrared Phys. Technol.* **1997**, *38*, 233.

(19) Kang, L.; Zhou, M. L.; Yao, J. Y.; Lin, Z. S.; Wu, Y. C.; Chen, C. T. *J. Am. Chem. Soc.* **2015**, *137*, 13049.

(20) (a) Kang, L.; Luo, S. Y.; Peng, G.; Ye, N.; Wu, Y. C.; Chen, C. T.; Lin, Z. *Inorg. Chem.* **2015**, *54*, 10533. (b) Lin, X. S.; Guo, Y. F.; Ye, N. *J. Solid State Chem.* **2012**, *195*, 172. (c) Zou, G. H.; Ye, N.; Huang, L.; Lin, X. S. *J. Am. Chem. Soc.* **2011**, *133*, 20001. (d) Feng, K.; Yin, W. L.; Lin, Z. H.; Yao, J. Y.; Wu, Y. C. *Inorg. Chem.* **2013**, *52*, 11503. (e) Christensen, A. N.; Rasmussen, S. E.; Karvonen, P.; Kjær, A.; Shapiro, R. H.; Westerdahl, A. *Acta Chem. Scand.* **1965**, *19*, 421. (f) Huang, Y.; Meng, X. G.; Gong, P. F.; Lin, Z. S.; Chen, X. G.; Qin, J. G. *J. Mater. Chem. C* **2015**, *3*, 9588. (g) Li, Y. J.; Wang, M.; Zhu, T. X.; Meng, X. G.; Zhong, C.; Chen, X. G.; Qin, J. G. *Dalton Trans.* **2012**, *41*, 763. (h) Ren, P.; Qin, J. G.; Chen, C. T. *Inorg. Chem.* **2003**, *42*, 8. (i) Wu, Q.; Huang, Y.; Meng, X. G.; Zhong, C.; Chen, X. G.; Qin, J. G. *Dalton Trans.* **2014**, *43*, 8899. (j) Zhang, G.; Qin, J. G.; Liu, T.; Zhu, T. X.; Fu, P. Z.; Wu, Y. C.; Chen, C. T. *Cryst. Growth Des.* **2008**, *8*, 2946.

(21) (a) Lin, X. S.; Zhang, G.; Ye, N. *Cryst. Growth Des.* **2009**, *9*, 1186. (b) Feng, K.; Shi, Y. G.; Yin, W. L.; Wang, W. D.; Yao, J. Y.; Wu, Y. C. *Inorg. Chem.* **2012**, *51*, 11144. (c) Aitken, J. A.; Larson, P.; Mahanti, S. D.; Kanatzidis, M. G. *Chem. Mater.* **2001**, *13*, 4714. (d) Marking, G. A.; Kanatzidis, M. G. *J. Alloys Compd.* **1997**, *259*, 122. (e) Zhang, X.; Kanatzidis, M. G.; Hogan, T.; Kannewurf, C. R. *J. Am. Chem. Soc.* **1996**, *118*, 693. (f) Zhou, M. L.; Kang, L.; Yao, J. Y.; Lin, Z. S.; Wu, Y. C.; Chen, C. T. *Inorg. Chem.* **2016**, *55*, 3724.

(22) Jang, J. I.; Haynes, A. S.; Saouma, F. O.; Otieno, C. O.; Kanatzidis, M. G. *Opt. Mater. Express* **2013**, *3*, 1302.

(23) Chung, I.; Song, J. H.; Jang, J. I.; Freeman, A. J.; Kanatzidis, M. G. *J. Solid State Chem.* **2012**, *195*, 161.

DOI: 10.1021/jacs.6b03734
J. Am. Chem. Soc. 2016, 138, 7422−7428

(24) Luo, Z. Z.; Lin, C. S.; Zhang, W. L.; Zhang, H.; He, Z. Z.; Cheng, W. D. *Chem. Mater.* **2014**, *26*, 1093.
(25) Bai, L.; Lin, Z. S.; Wang, Z. Z.; Chen, C. T.; Lee, M. H. *J. Chem. Phys.* **2004**, *120*, 8772.
(26) (a) Isaenko, L.; Vasilyeva, I.; Merkulov, A.; Yelisseyev, A.; Lobanov, S. *J. Cryst. Growth* **2005**, *275*, 217. (b) Fossier, S.; Salaun, S.; Mangin, J.; Bidault, O.; Thenot, I.; Zondy, J. J.; Chen, W. D.; Rotermund, F.; Petrov, V.; Petrov, P.; Henningsen, J.; Yelisseyev, A.; Isaenko, L.; Lobanov, S.; Balachninaite, O.; Slekys, G.; Sirutkaitis, V. *J. Opt. Soc. Am. B* **2004**, *21*, 1981. (c) Tyazhev, A.; Vedenyapin, V.; Marchev, G.; Isaenko, L.; Kolker, D.; Lobanov, S.; Petrov, V.; Yelisseyev, A.; Starikova, M.; Zondy, J. J. *Opt. Mater.* **2013**, *35*, 1612.
(27) Chung, I.; Kim, M. G.; Jang, J. I.; He, J. Q.; Ketterson, J. B.; Kanatzidis, M. G. *Angew. Chem., Int. Ed.* **2011**, *50*, 10867.
(28) Yao, J. Y.; Mei, D. J.; Bai, L.; Lin, Z. S.; Yin, W. L.; Fu, P.; Wu, Y. C. *Inorg. Chem.* **2010**, *49*, 9212.
(29) Mei, D. J.; Yin, W. L.; Feng, K.; Lin, Z. S.; Bai, L.; Yao, J. Y.; Wu, Y. C. *Inorg. Chem.* **2012**, *51*, 1035.
(30) Lekse, J. W.; Moreau, M. A.; McNerny, K. L.; Yeon, J.; Halasyamani, P. S.; Aitken, J. A. *Inorg. Chem.* **2009**, *48*, 7516.
(31) Zhang, G.; Li, Y. J.; Jiang, K.; Zeng, H. Y.; Liu, T.; Chen, X. G.; Qin, J. G.; Lin, Z. S.; Fu, P. Z.; Wu, Y. C.; Chen, C. T. *J. Am. Chem. Soc.* **2012**, *134*, 14818.
(32) Wu, Q.; Meng, X. G.; Zhong, C.; Chen, X. G.; Qin, J. G. *J. Am. Chem. Soc.* **2014**, *136*, 5683.
(33) Burton, L. A.; Colombara, D.; Abellon, R. D.; Grozema, F. C.; Peter, L. M.; Savenije, T. J.; Dennler, G.; Walsh, A. *Chem. Mater.* **2013**, *25*, 4908.
(34) Brant, J. A.; Clark, D. J.; Kim, Y. S.; Jang, J. I.; Zhang, J.; Aitken, J. A. *Chem. Mater.* **2014**, *26*, 3045.
(35) Jorgens, S.; Johrendt, D.; Mewis, A. *Z. Anorg. Allg. Chem.* **2002**, *628*, 1765.
(36) Sheldrick, G. M. *SHELXTL*; Bruker Analytical X-ray Instruments, Inc.: Madison, WI, 2008.
(37) Spek, A. L. *J. Appl. Crystallogr.* **2003**, *36*, 7.
(38) Kortüm, G. *Reflectance Spectroscopy*; Springer Verlag: New York, 1969.
(39) Kurtz, S. K.; Perry, T. T. *J. Appl. Phys.* **1968**, *39*, 3798.
(40) Clark, S. J.; Segall, M. D.; Pickard, C. J.; Hasnip, P. J.; Probert, M. J.; Refson, K.; Payne, M. C. *Z. Kristallogr. - Cryst. Mater.* **2005**, *220*, 567.
(41) Blöchl, P. E.; Jepsen, O.; Andersen, O. K. *Phys. Rev. B: Condens. Matter Mater. Phys.* **1994**, *49*, 16223.
(42) (a) Godby, R. W.; Schluter, M.; Sham, L. J. *Phys. Rev. B: Condens. Matter Mater. Phys.* **1988**, *37*, 10159. (b) Wang, C. S.; Klein, B. M. *Phys. Rev. B: Condens. Matter Mater. Phys.* **1981**, *24*, 3417.
(43) Aversa, C.; Sipe, J. E. *Phys. Rev. B: Condens. Matter Mater. Phys.* **1995**, *52*, 14636.
(44) Lin, J.; Lee, M. H.; Liu, Z. P.; Chen, C.; Pickard, C. J. *Phys. Rev. B: Condens. Matter Mater. Phys.* **1999**, *60*, 13380.
(45) (a) Devi, M. S.; Vidyasagar, K. *Dalton Trans.* **2002**, *9*, 2092. (b) Brant, J. A.; Clark, D. J.; Kim, Y. S.; Jang, J. I.; Weiland, A.; Aitken, J. A. *Inorg. Chem.* **2015**, *54*, 2809. (c) Brant, J. A.; de la Cruz, C. D.; Yao, J. L.; Douvalis, A. P.; Bakas, T.; Sorescu, M.; Aitken, J. A. *Inorg. Chem.* **2014**, *53*, 12265. (d) Choudhury, A.; Ghosh, K.; Grandjean, F.; Long, G. J.; Dorhout, P. K. *J. Solid State Chem.* **2015**, *226*, 74. (e) Chung, I.; Kanatzidis, M. G. *Chem. Mater.* **2014**, *26*, 849. (f) Devlin, K. P.; Glaid, A. J.; Brant, J. A.; Zhang, J. H.; Srnec, M. N.; Clark, D. J.; Soo Kim, Y.; Jang, J. I.; Daley, K. R.; Moreau, M. A.; Madura, J. D.; Aitken, J. A. *J. Solid State Chem.* **2015**, *231*, 256. (g) Lekse, J. W.; Leverett, B. M.; Lake, C. H.; Aitken, J. A. *J. Solid State Chem.* **2008**, *181*, 3217. (h) Olivier, F. J.; Philippot, E.; Ribes, M.; Maurin, M. *C. R. Acad. Sci., Ser. IIc: Chim.* **1972**, *274*, 1185.
(46) Palchik, O.; Marking, G. M.; Kanatzidis, M. G. *Inorg. Chem.* **2005**, *44*, 4151.
(47) Olivier-Fourcade, J.; Ribes, M.; Philippot, E.; Maurin, M. *C. R. Acad. Sci., Ser. IIc: Chim.* **1971**, *272*, 1964.
(48) Klepp, K. O.; Fabian, F. *Z. Naturforsch., B: J. Chem. Sci.* **1999**, *54*, 1499.
(49) Morris, C. D.; Li, H.; Jin, H.; Malliakas, C. D.; Peters, J. A.; Trikalitis, P. N.; Freeman, A. J.; Wessels, B. W.; Kanatzidis, M. G. *Chem. Mater.* **2013**, *25*, 3344.
(50) Lin, H.; Zhou, L. J.; Chen, L. *Chem. Mater.* **2012**, *24*, 3406.

DOI: 10.1021/jacs.6b03734
J. Am. Chem. Soc. 2016, 138, 7422−7428